

RSC Advances



This is an *Accepted Manuscript*, which has been through the Royal Society of Chemistry peer review process and has been accepted for publication.

Accepted Manuscripts are published online shortly after acceptance, before technical editing, formatting and proof reading. Using this free service, authors can make their results available to the community, in citable form, before we publish the edited article. This *Accepted Manuscript* will be replaced by the edited, formatted and paginated article as soon as this is available.

You can find more information about *Accepted Manuscripts* in the [Information for Authors](#).

Please note that technical editing may introduce minor changes to the text and/or graphics, which may alter content. The journal's standard [Terms & Conditions](#) and the [Ethical guidelines](#) still apply. In no event shall the Royal Society of Chemistry be held responsible for any errors or omissions in this *Accepted Manuscript* or any consequences arising from the use of any information it contains.

Graphical Abstract

Fluorinated Polyhedral Oligomeric Silsesquioxane

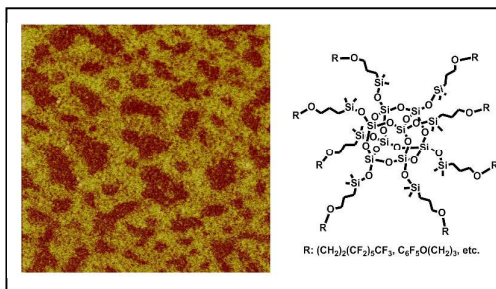
Xiaobai Wang,[†] Qun Ye,[†] Jing Song,[†] Ching Mui Cho,[†] Chaobin He,^{†,‡} Jianwei Xu^{†,§,*}

[†] Institute of Materials Research and Engineering, A*STAR (Agency for Science, Technology and Research), 3 Research Link, Republic of Singapore 117602

[‡] Department of Materials Science & Engineering, National University of Singapore, 5 Engineering Drive 2, Republic of Singapore 117576

[§] Department of Chemistry, National University of Singapore, 3 Science Drive 3, Singapore 117543

A series of fluorinated polyhedral oligomeric silsesquioxanes (POSS) oil were readily prepared *via* hydrosilylation reaction.



Fluorinated Polyhedral Oligomeric Silsesquioxane

Xiaobai Wang,[†] Qun Ye,[†] Jing Song,[†] Ching Mui Cho,[†] Chaobin He,^{†,‡} Jianwei Xu^{†,*}

[†] Institute of Materials Research and Engineering, A*STAR (Agency for Science, Technology and Research), 3 Research Link, Republic of Singapore 117602

[‡] Department of Materials Science & Engineering, National University of Singapore, 5 Engineering Drive 2, Republic of Singapore 117576

jw-xu@imre.a-star.edu.sg

Abstract

A series of fluorinated polyhedral oligomeric silsesquioxanes (POSS) derivatives were prepared *via* hydrosilylation reaction and they were characterized by ¹H, ¹³C, ²⁹Si and ¹⁹F nuclear magnetic resonance (NMR) spectroscopy and elemental analysis. The thermal stability of POSS derivatives was studied using thermogravimetric analyzer (TGA) and they exhibited high decomposition temperatures ranging from 327 to 380 °C in air and inert atmosphere. At ambient temperature, fluorinated POSS (FluoroPOSS) compounds **3a-b** and **3d-e** appear as fluidic oils with dynamic viscosity of 140–430 mPas and it is noteworthy to mention that **3a**, **3d** and **3e** do not solidify even below -80 °C. The thermal aging experiments of these FluoroPOSS oils were examined, and results revealed that these oils exhibited excellent long-term thermal stability with minimal weight loss over 48 hours in air, rendering them to be the promising lubricant candidates for unique application in a wide temperatures range from -80 to 300 °C. These fluorinated POSS derivatives have also shown potential in polymer surface modification as evidenced by the great increase in water contact angle from ~ 68° for neat hydrophilic PMMA film to 94-105° for the blended film with 5 wt.% fluorinated derivatives. The rise in water contact angle is likely to be due to migration of hydrophobic POSS core from interior to surface, which has been observed by atomic force microscopy (AFM).

Introduction

Polyhedral oligomeric silsesquioxane (POSS) molecules¹⁻⁴ comprise silicon and oxygen atoms which are alternatively linked into a well-defined nano-sized rigid regular structure with the silicon atoms at the corners. It has been demonstrated as a versatile platform⁵ for a variety of functional nanomaterials, such as organic light emitting diode materials⁶, liquid crystal materials⁷, biomaterials⁸⁻¹⁰, catalyst support¹¹, and hybrid polymers^{12,13}. The corner silicon atoms are allowed to be modified with suitable functional groups, such as alkenyl and Si-H groups, which enable it to be further functionalized *via* hydrosilylation in the presence of platinum catalyst¹⁴, to offer exceptional organic-inorganic hybrid structures with specific properties.

Out of the vast library of POSS based materials, fluorinated POSS¹⁵, in which the corner substituents are perfluoroalkyl chains, has drawn significant attention due to their intriguingly low solid-surface energy¹⁶ as highly hydrophobic¹⁷⁻²⁰ and superoleophobic materials²¹. Blending of fluorinated POSS into functional polymers, e.g., poly (methyl methacrylate) (PMMA)²² and cross-linked poly(ethylene glycol) diacrylate²³, is witnessed as an efficient way to tune the hydrophobicity of the coated film and to prepare hygro-responsive membrane for effective oil-water separation, respectively. This novel class of polyhedral fluorinated materials is also envisaged to function as high performance lubricant oils and can be used in their original form or formulated into greases for specific applications under highly demanding conditions²⁴⁻²⁶, for example, in the chemical, electronic, military, nuclear, and other industries. Nevertheless, fluidic POSS based derivatives that are suitable as lubricating base oil have rarely been reported.²⁷ This prompts us to prepare fluidic fluorinated POSS based oils with suitable physical properties as high performance lubricants under harsh conditions.²⁸

Fluorinated lubricants in general have extremely high thermal and chemical stability such as non-combustible and exceptionally stable to oxygen. They are chemically inert and highly resistant to chemicals. This type of lubricant usually exhibit excellent lubricity over a wide of temperature range. Moreover, they show low vapor pressure and thus have low weight loss at high temperature environment. However, the wide application of fluorinated lubricant is hampered by their relatively high cost compared with the petroleum originated lubricants.²⁹

Inclusion of a POSS core in this type of lubricant, leads to significant reduction of weight percentage of fluorine, and may effectively lower the cost, and extend their applications. The present paper describes the preparation method of fluorinated octameric POSS derivatives from the POSS precursor which contains reactive functional groups, $-\text{O}(\text{Me})_2\text{Si}-\text{H}$, at the corners. This functional group Si-H allows for feasible chemical modification by hydrosilylation in the presence of suitable platinum catalyst to offer a wide range of POSS compounds with various specifically designed properties. Their physical properties and tribological behavior are characterized herein. In addition, blending of the POSS oils with PMMA is also carried out to tune the hydrophobicity of the PMMA film.

Experimental sections

Synthesis of fluorinated POSS

Octameric silsesquioxanes octakis(hydrodimethylsiloxy) octasilsesquioxane (**1**) ($\text{Si}_8\text{O}_{12}(\text{OSi}(\text{Me})_2\text{H})_8$) was purchased from Hybrid Plastics. All non-fluorinated chemicals and solvents (AR grade) were bought from Sigma Aldrich and all fluorine-containing chemicals were bought from ABCR GmbH & Co. KG. They were used as received unless stated. Fluorinated alkene intermediates were synthesized according to the reference³⁰ with slight modification. The intermediates were obtained as colorless liquid. The fluorinated POSS derivatives were obtained by hydrosilation reaction between $\text{Si}_8\text{O}_{12}(\text{OSi}(\text{Me})_2\text{H})_8$ and fluorinated alkenes.

Synthesis of fluorinated alkenes General procedures

Perfluorinated alcohol or phenol (38.4 mmol) was added into a sodium hydroxide aqueous solution (60 mL, 30% v:v) and was stirred for 30 min at 40 °C, followed by the addition of Aliquat[®]336 (methyltrioctyl ammonium chloride) as catalyst. Allyl bromide (40.0 g, 331.0 mmol) was then added into the above mixture. The reaction was maintained at 40°C and allowed to stir overnight. After the reaction was completed, the organic layer was separated and the water layer was extracted with chloroform (30 mL × 3). The organic layer was combined with chloroform, washed with water (40 mL × 4) and dried with anhydrous sodium sulfate. After the

drying agent was removed by filtration, chloroform was evaporated by rotary evaporator. The product was obtained as a colorless liquid by vacuum distillation.

8-(allyloxy)-1,1,1,2,2,3,3,4,4,5,5,6,6-tridecafluorooctane (**2a**): yield, 50%; ^1H NMR (CDCl_3 , 400 MHz) δ (ppm): 5.90 (m, 1H), 5.25 (m, 2H), 4.01 (d, 2H), 3.73 (t, 2H), 2.42 (m, 2H).

8-(allyloxy)-1,1,1,2,2,3,3,4,4,5,5,6,6,7,7-pentadecafluorooctane (**2b**): yield, 69%; ^1H NMR (CDCl_3 , 400 MHz) δ (ppm): 5.90 (m, 1H), 5.24 (m, 2H), 4.00 (d, 2H), 3.72 (t, 2H), 2.41 (m, 2H).

9-(allyloxy)-1,1,1,2,2,3,3,4,4,5,5,6,6, 7,7-pentadecafluorononane (**2c**): yield, 64%; ^1H NMR (CDCl_3 , 400 MHz) δ (ppm): 5.88 (m, 1H), 5.29 (m, 2H), 4.16 (d, 2H), 3.92 (t, 2H).

1,1,1,3,3,4,4,6,6,7,7,9,9, tridecafluoro-2,5,8,11-tetraoxatetradec-13-ene (**2d**): yield, 79%; ^1H NMR (CDCl_3 , 400 MHz) δ (ppm): 5.87 (m, 1H), 5.28 (m, 2H), 4.15 (d, 2H), 3.81 (t, 2H). EI-MS: 437.0 (m/e), Anal. Calcd for **2d** ($\text{C}_{10}\text{H}_7\text{F}_{13}\text{O}_4$): C, 27.41; H, 1.61; Found: C 27.49; H, 1.49.

1-(allyloxy)-2,3,4,5,6-pentafluorobenzene (**2e**): yield, 64%; ^1H NMR (CDCl_3 , 400 MHz) δ (ppm): 6.02 (m, 1H), 5.35 (m, 2H), 4.67 (d, 2H).

Synthesis of fluorinated octameric silsesquioxanes

A portion of compound **1** (1.0 g, 0.98 mmol) was placed into a three-necked round-bottom flask equipped with a magnetic stirrer together with 2 mL of dry toluene. **2a-2e** (9.8 mmol) was added to POSS and the mixture was stirred and purged with pure nitrogen gas for half an hour at 40 °C. A catalytic amount of platinum divinyltetramethyldisiloxane complex was added. The mixture was then heated up to 80°C and maintained at this temperature for 12 hours, after which the reaction mixture was subject to NMR analysis. The characteristic NMR signals of the multiple peaks of Si-H in POSS starting materials at 4.73 (m, 4.74 – 4.72) ppm disappeared, indicating the completeness of the reaction. The crude product was purified by column chromatography (Silica gel; 100% chloroform), and the last spot was collected.

3a, 3.7 g; yield, 89%. ^1H NMR (CDCl_3 , 400 MHz): δ (ppm) 3.68 (t, 16H), 3.40 (t, 16H), 2.37 (m, 16H), 1.64 (m, 16H), 0.60 (m, 16H) 0.14 (s, 48H). ^{13}C NMR (CDCl_3 , 100 MHz) δ (ppm) 120.7(m), 119.0(m), 118.2(m), 116.1(m), 113.9(m), 110.1(m), 108.6(m), 74.2, 62.8, 31.9 (t, $J = 21.4$ Hz), 23.4, 14.0. -0.2. ^{29}Si NMR (CDCl_3 , 79.5 MHz) δ (ppm) 13.01, -108.82. ^{19}F NMR (CDCl_3 , 276.5 MHz) δ (ppm) -81.0 (t, 24F, $J = 7.5$ Hz), -113.6 (t, 16F, $J = 9.4$ Hz), -122.1 (br, 16F), -123.0 (br, 16F), -123.8 (br, 16F), -126.3 (m, 16 F). Anal. Calcd for **3a** ($\text{C}_{104}\text{H}_{128}\text{F}_{104}\text{O}_{28}\text{Si}_{16}$): C, 29.38; H, 3.03; Found: C 29.78; H, 2.84.

3b, 3.6 g; yield, 81%. ^1H NMR (CDCl_3 , 400 MHz) δ (ppm) 3.89 (t, 16H), 3.54(t, 16H), 1.64 (m, 16H), 0.59 (m, 16H), 0.14 (s, 48H). ^{13}C NMR (CDCl_3 , 100 MHz) δ (ppm) 121.4(m), 118.7(m), 116.0(m), 113.7(m), 111.4(m), 108.8(m), 76.0, 68.1 (t, $J = 24.9$ Hz), 23.4, 13.7, -0.3. ^{29}Si NMR (CDCl_3 , 79.5 MHz) δ (ppm) 13.19, -108.84. ^{19}F NMR (CDCl_3 , 276.5 MHz) δ (ppm) -81.0 (t, 24F, $J = 7.0$ Hz), -119.8 (m, 16F), -122.3 (m, 32F), -123.6 (m, 16F), -123.8 (br, 16F), -126.4 (m, 16 F). Anal. Calcd for **3b** ($\text{C}_{104}\text{H}_{112}\text{F}_{120}\text{O}_{28}\text{Si}_{16}$): C, 27.52; H, 2.49; Found: C 27.58; H, 2.82.

3c, 3.4 g, yield, 70%. ^1H NMR (CDCl_3 , 400 MHz) δ (ppm) 3.68 (t, 16H), 3.40 (t, 16H), 2.37 (m, 16H), 1.61 (m, 16H), 0.60 (m, 16H), 0.14 (s, 48H). ^{13}C NMR (CDCl_3 , 100 MHz) δ (ppm) 120.7(m), 118.2(m), 115.7(m), 113.9(m), 111.2(m), 108.6(m), 74.2, 62.8, 31.8 (t, $J = 21.5$ Hz), 23.4, 14.0, -0.2. ^{29}Si NMR (CDCl_3 , 79.5 MHz) δ (ppm) 13.13, -108.87. ^{19}F NMR (CDCl_3 , 276.5 MHz) δ (ppm) -80.9 (t, 24F, $J = 7.0$ Hz), -113.6 (t, 16F, $J = 9.0$ Hz), -121.8(m, 16F), -122.1 (br, 16F), -122.9 (br, 16F), -123.8 (br, 16F), -126.3 (m, 16F). Anal. Calcd for **3c** ($\text{C}_{112}\text{H}_{128}\text{F}_{120}\text{O}_{28}\text{Si}_{16}$): C, 28.92; H, 2.77; Found: C 28.76; H, 2.87.

3d, 1.7 g, yield, 37%. ^1H NMR (CDCl_3 , 400 MHz) δ (ppm) 3.77 (t, 16H), 3.54 (t, 16H), 1.61 (m, 16H), 0.58 (m, 16H), 0.13 (s, 48H). ^{13}C NMR (CDCl_3 , 100 MHz) δ (ppm) 125.7(m), 122.9(m), 120.8(m), 120.1(m), 117.1(m), 114.3(m), 111.6(m), 75.7, 69.9 (t, $J = 30.4$ Hz), 23.4, 13.6, -0.2. ^{29}Si NMR (CDCl_3 , 79.5 MHz) δ (ppm) 13.12, -108.87. ^{19}F NMR (CDCl_3 , 276.5 MHz) δ (ppm) -55.6 (t, 16F, $J = 6.3$ Hz), -77.9 (t, 16F, $J = 9.7$ Hz), -88.7 ~ -89.0 (m, 56F), -90.8 (t, 16F, $J = 6.2$ Hz). Anal. Calcd for **3d** ($\text{C}_{96}\text{H}_{112}\text{F}_{104}\text{O}_{52}\text{Si}_{16}$): C, 25.49; H, 2.50; Found: C 25.97; H, 2.80.

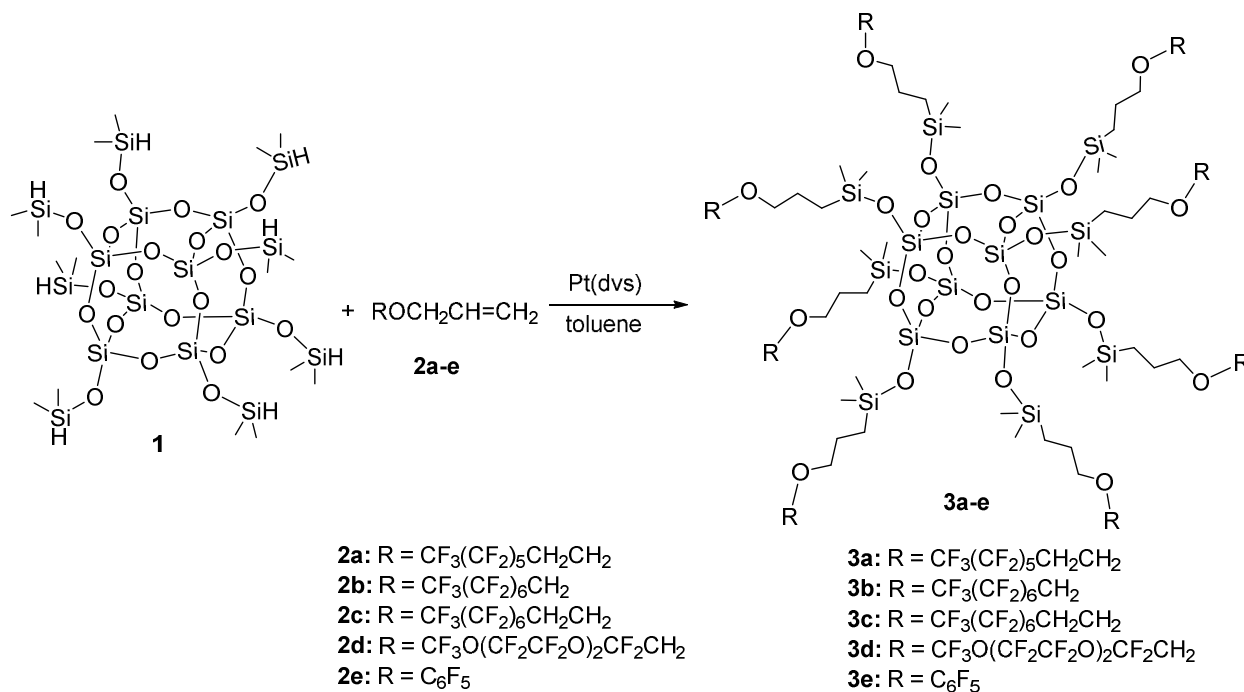
3e, 0.94 g, yield, 34%. The product was pure enough for further chemical analysis. ^1H NMR (CDCl_3 , 400 MHz) δ (ppm): 4.08 (m, br, 16H), 1.80 (m, 16H), 0.71 (m, 16H), 0.16 (m, 48H). ^{13}C NMR (CDCl_3 , 400 MHz) δ (ppm): 143.3 (m), 140.8(m), 139.6(m), 137.1(m), 78.4, 23.9, 13.6, -0.2. ^{29}Si NMR (CDCl_3 , 79.5 MHz) δ (ppm): 12.76, -108.90. ^{19}F NMR (CDCl_3 , 276.5 MHz) δ (ppm) -157.0 (br, 16F), -163.7(br, 16F), -164.0 (br, 8F). Anal. Calcd for **3e** ($\text{C}_{88}\text{H}_{96}\text{F}_{40}\text{O}_{28}\text{Si}_{16}$): C, 37.60; H, 3.44; Found: C 37.20; H, 3.28.

Results and Discussion

Synthesis and chemical characterization

The synthetic routes leading to fluorinated POSS oils **3a–e** are shown in Scheme 1. Synthesis of fluorinated precursors **2a–e** was followed the reference.^{30a} An alkenyl terminal group were prepared by reacting perfluorinated alcohol with excess allyl bromide in the presence of sodium hydroxide. Different fluorinated moieties including fluorinated ether chains, fluorinated oligoether chains, fluoroalkyl chains, perfluoroaromatic units are prepared in this way. A hydrosilylation reaction between POSS compound **1** with compounds **2a–e** was performed in dry toluene at room temperature with the catalyst platinum divinyltetramethyldisiloxane complex ($\text{Pt}(\text{dvs})$) (Scheme 1). An excess of **2a–e** was used to ensure that the hydrosilylation was complete. Crude products were purified by silica gel column chromatography to afford pure **3a–e**. All fluorinated POSS compounds **3a–e** were characterised by ^1H , ^{13}C , ^{29}Si and ^{19}F NMR spectroscopies, and elemental analysis. All POSS compounds except **3e** are α -addition dominant product. For **3e**, the formation of a nearly equal amount of α - and β -addition products was observed most probably due to strong electron withdrawing characteristics of pentafluorophenyl group.^{30b} The disappearance of the Si–H absorption at 2142 cm^{-1} in FT-IR spectra and the signal at 4.7 ppm which is assigned to Si–H in ^1H NMR spectra, in combination with ^{13}C and ^{29}Si NMR spectra, confirm exactly eight-fold substitutions. As an example, ^1H NMR and ^{29}Si NMR spectra of **3a** are given in Fig. 1 and 2, respectively. Two pairs of triplets at $\delta = 3.68$ ppm and were assigned to two OCH_2 groups (d and e). Other three multiplets at $\delta = 2.37$, 1.59 and 0.60 ppm corresponded to $-\text{OCH}_2\text{CH}_2\text{CF}_2$ (f), $\text{Si}(\text{Me})_2\text{CH}_2\text{CH}_2\text{CH}_2\text{O}-$ (c), $\text{Si}(\text{Me})_2\text{CH}_2\text{CH}_2\text{CH}_2\text{O}-$ (b), respectively. A pseudo-triplet at $\delta = 0.6$ ppm and the absence of signals at $\delta = 2.5$ ppm both indicate that the addition of the Si–H bond to the alkene **2a–e** ($\text{CH}_2^\beta=\text{CH}^\alpha\text{-R}$) affords regiospecific β -addition products, consistent with reported examples.^{31,32} In the ^{29}Si NMR

spectrum of **3a**, two singlets at δ around 13 and -108 ppm, which are assigned to the Si atom on the side chains and the cage Si atom, respectively, were observed, indicating the octameric cage structure is intact during the synthesis. Fluorinated POSS **3a–b** and **3d–e** are colourless or very light yellow oil at room temperature and are soluble in common organic solvents such as tetrahydrofuran, chloroform, etc.



Scheme 1. Synthesis of fluorinated POSS **3a-e**.

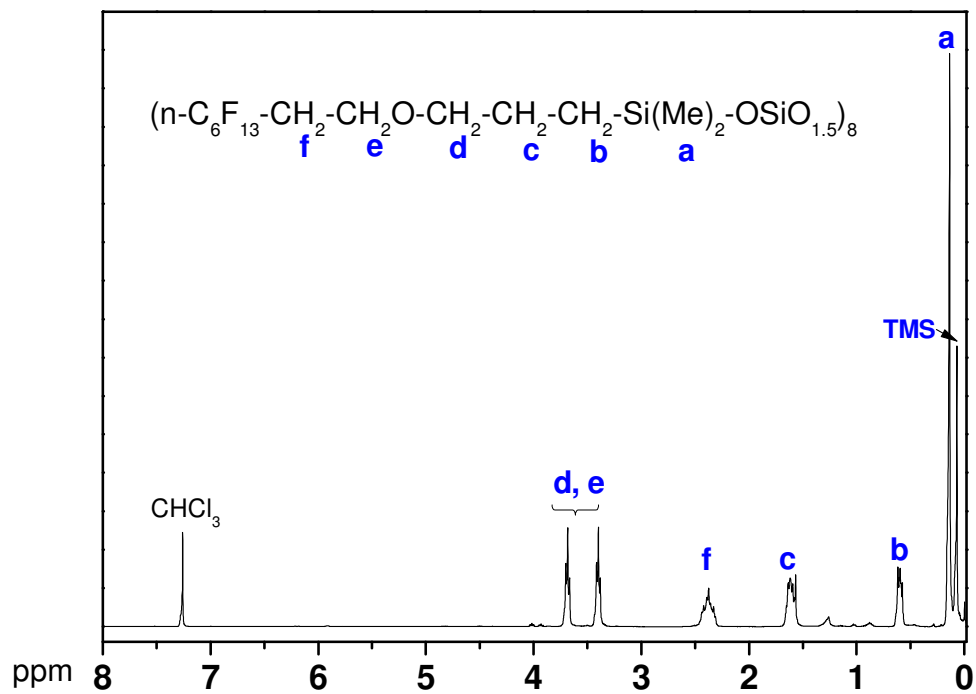


Figure 1: ¹H spectrum of compound **3a** in CDCl₃ at room temperature.

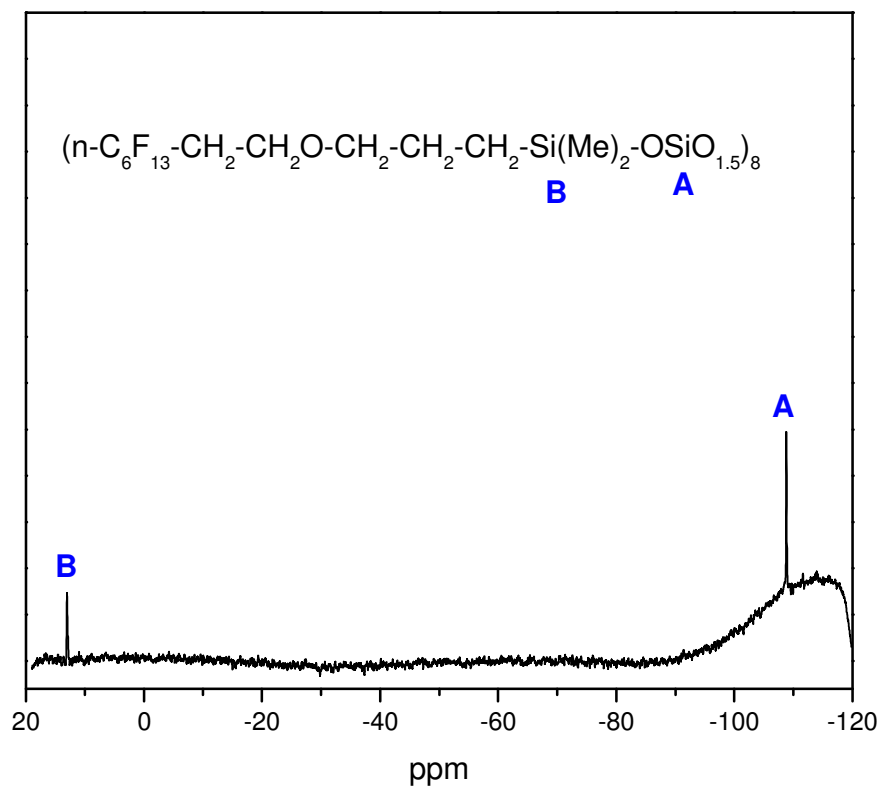


Figure 2. ²⁹Si NMR spectrum of fluorinated POSS **3a** in CDCl₃ at room temperature.

Thermal stability study

Thermal gravimetric analysis (TGA) experiments were conducted to observe the thermal stability of the fluorinated POSS oils. The decomposition temperature is defined as the temperature at which the 5% weight loss occurs. The results are summarized in Table 1 together with the freezing points and melting points. The synthesized POSS derivatives display relatively high decomposition temperatures. The decomposition temperatures of all five POSS molecules are between 327-380 °C in air and in nitrogen. Differential scanning calorimetry (DSC) experiments are conducted and no notable phase transitions are observed down to -80 °C for **3a**, **3d** and **3e**. Three POSS derivatives (**3a**, **3d** and **3e**) show intriguing freezing and melting points of less than -80 °C (Table 1), indicating that these fluorinated lubricants have a wide operation temperature range.

Table 1 Summary of decomposition temperature, freezing point, melting point and thermal weight loss of fluorinated POSS **3a-e**

Fluoro POSS	MW	F(%)	T _d ^a in N ₂ (°C)	T _d ^a in air (°C)	Freezing point (°C)	Melting point (°C)	Evaporation loss ^b (%)
3a	4251.3	46.5	366	359	< -80	< -80	55.6
3b	4539.2	50.2	363	370	-50	20	19.9
3c	4651.4	49.0	382	379	0	45	-- ^c
3d	4523.1	43.7	327	338	< -80	< -80	-- ^c
3e	2811.0	27.0	354	380	< -80	< -80	1.8

^aT_d is defined as the temperature at which 5% weight loss occurs. ^bEvaporation loss is defined as the weight loss after the oil is continuously heated at 218 °C for 48h. ^c. Not tested.

Some essential features of high temperature lubricant composition include low evaporation loss and no formation of deposits or varnish when exposed to high temperature environment. In order to measure the evaporation loss of the lubricant at a certain high temperature, a lubricant sample is maintained in an oven at 218 °C for 48 h and the weight loss is then determined. As shown in Table 1, the POSS oils **3e** exhibit the best thermal behavior with mass loss less than 2% after being heated at 218 °C for 48h and no deposit or varnish observed. The observed low

evaporation loss of **3e** is mainly ascribed to the strong aromatic π - π intermolecular interaction compared with other fluorinated POSS oils (*vide infra*).

Viscosity measurement

Similar to traditional lubricants, the viscosity of POSS derivatives has shown to behave like that of a Newtonian liquid (Figure 3). The dynamic viscosities for all FluoroPOSS lubricant are measured and the data are summarized in Table 2. As usual, viscosities decrease with the increase of temperature. The dynamic viscosity of FluoroPOSS lubricants is in the range of 0.05-0.43 Pas at 25°C. The dynamic viscosity drops to 0.29-0.049 Pas at 40 °C and further goes down to 0.017-0.019 Pas at 100 °C as shown in Table 2. As is witnessed by the dynamic viscosity study, the sample **3e** has a much higher viscosity compared with the rest of fluorinated POSS samples and this explains the much lower evaporation loss of **3e** under high temperature.

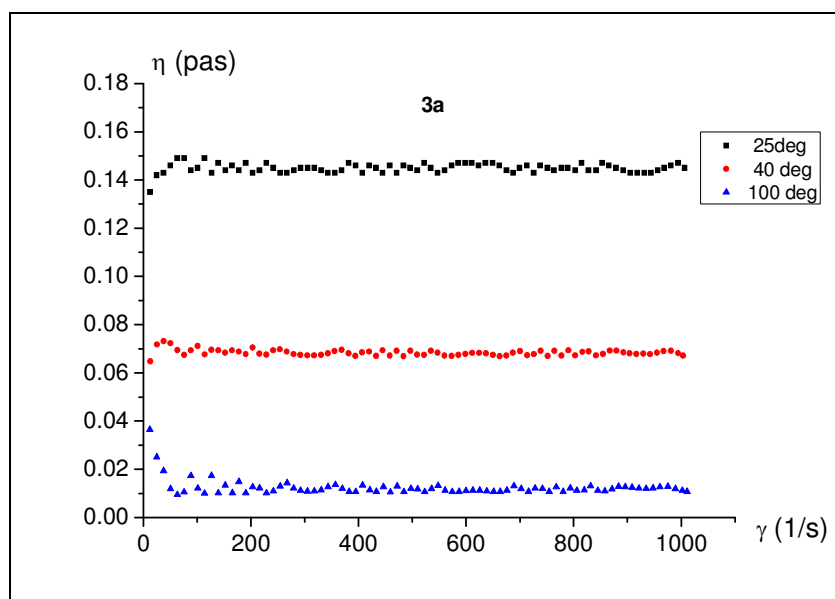


Figure 3. The dynamic viscosity behaviors for **3a**: (black) 25 °C, (red) 40 °C, and (blue) 100 °C.

Table 2. Viscosity data for selected FluoroPOSS lubricants

F-POSS	Viscosity (mPas) at 25°C	Viscosity (mPas) at 40°C	Viscosity (mPas) at 100°C
3a	140	65	13

3b	220	88	56
3c^a	-	-	22
3d	76	68	34
3e	430	290	120

^a: solid at room temperature.

Blend study with PMMA

Water contact angle is measured to investigate the hydrophobic properties of the FluoroPOSS molecules. Poly(methyl methacrylate) (PMMA) is a medium hydrophilic material with a contact angle of 65-72°. ^{33,34} PMMA has wide applications in coatings, adhesives, medicals and implants. However, water absorption by PMMA would lead to the hydrolytic degradation and thus have detrimental effect on its durability. Inclusion of hydrophobic materials and subsequent increase of water contact angle offers an opportunity to retard the degradation of PMMA materials. The water contact angles of PMMA with 5% POSS derivatives **3a-e** at 25 °C are measured and data are summarized in Table 3. The water droplet images of PMMA and PMMA/5% **3a** are showed in Figure 4. The water contact angle greatly increases from 68° for pure PMMA to more than 90° for PMMA with 5% weight fluorinated POSS loading. For comparison, the water contact angle of PMMA with a same loading of a non-fluorinated POSS material [n-C₈H₁₇O(CH₂)₃Si(Me)₂OSiO_{1.5}]₈ is measured. Only a contact angle of 81.2° is observed, suggesting that the introduction of fluorine atoms to POSS structures leads to a significant increase in water contact angle.

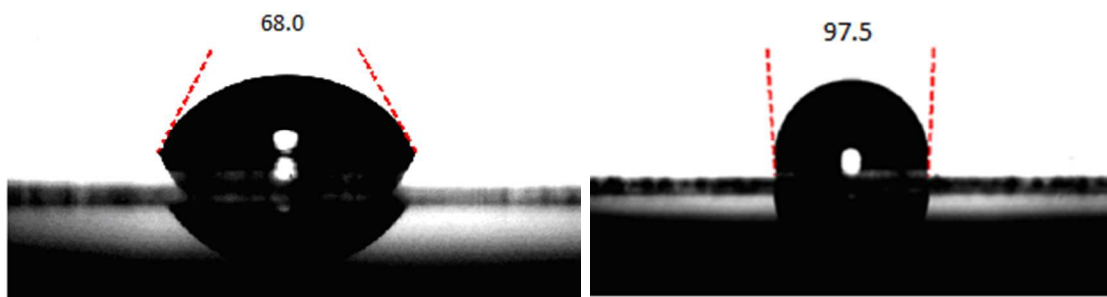


Figure 4. Water droplet images of PMMA and PMMA/5% **3a**

TABLE 3. Water contact angle of POSS/PMMA blends

Composition	Contact angle
PMMA/5% [n-C ₈ H ₁₇ O(CH ₂) ₃ Si(Me) ₂ OSiO _{1.5}] ₈	81.2
PMMA/5% 3a	97.5
PMMA/5% 3b	99.3
PMMA/5% 3c	99.2
PMMA/5% 3d	94.4
PMMA/5% 3e	104.6
PMMA	68.0

By varying the mass fraction of specific POSS molecules with PMMA, the systematically change of surface energy of blend thin films have been shown in previous study.¹⁷ With increasing the fraction of FluoroPOSS in the blend films, the surface energy was decreased. To further elucidate the surface morphology and mechanical properties of blend films in a micro or nanometer scale, atomic force microscopy (AFM) method was applied. The AFM tapping mode phase images of the spin-coated FluoroPOSS-PMMA blends are shown in Figure 5. Phase image records the phase shift signal which can be related local energy dissipation by the tip sample interaction. Without FluoroPOSS, a featureless phase image is obtained (Figure 5a). RMS roughness measured on a 5×5 μm² area was 0.56 nm. With increasing FluoroPOSS fraction in the blend film (0.3 mg/mL), nano scale phase separated domains are observed (Figure 5b). The domains size ranges from 600 nm - 1000 nm with the increased roughness 1.02 nm. The phase contrast may show the dispersion of FluoroPOSS molecules in PMMA due to different surface energy of materials. With increasing the FluoroPOSS concentration to 1 mg/mL, the surface tends to show a tiny granular morphology. Between the granular structures, the film appears continuous. Meanwhile, the surface roughness increased to 2.24 nm. These images indicate FluoroPOSS material migrated to enrich the top surface in preference to the PMMA. The driving forces for this surface enrichment can be caused by difference in the surface free energies of the polymer components in order to minimize the polymer air surface tension.

Measurements of lateral friction forces have taken a central role in fundamental studies of tribology. The friction force measurement was performed in contact mode by scanning the tip in the direction orthogonal to the long cantilever. To evaluate frictional force, we analyzed line profiles of friction loops. The variation of averaged frictional forces as a function of the applied normal forces is shown in Figure 6. The measurements were performed using a Si₃N₄ probe tip with a scan velocity of 2 μm/s. Before friction measurements were made, force distance curves were captured and the set point adjusted to control the value of the normal force. In theory, a linear relationship between the later force and the normal force is

$$F_L = F_0 + \mu F_N \quad (\text{Eq. 1})$$

where F_0 is a constant friction force and μ is the normal friction coefficient. The value of F_0 usually correlates, but is not necessarily equal, to adhesion forces obtained from approaching-retracting measurements.

As is clear from these data, the frictional forces increase almost linearly with load for PMMA and low fraction FluoroPOSS polymer blends. The friction force shows non linearity at high load range for the high fraction FluoroPOSS polymer blend. The friction coefficient of PMMA, μ_{PMMA} , is 0.425. With a low POSS fraction (0.3 mg/mL), the film shows a decreased frictional coefficient, 0.409. However, with higher FluoroPOSS concentration (1 mg/mL), the friction coefficient increased to 1.265 accompanied by the increased the roughness. Similar observation is reported for a functionalized graphene oxide system.³⁵ The variation of friction coefficient can be understood by considering the various interactions at the tip substrate interface during contact. At the lower fraction of FluoroPOSS blend film (0.3mg/mL), the FluoroPOSS molecules tended to homogeneously disperse in the PMMA. The lower friction obtained is likely due to decrease in surface energy of blends. As PMMA is a hydrophilic material, it is thus easy to trap the moisture, resulting in inducing additional capillary force between the tip and sample. With increase of the fraction of FluoroPOSS in the blend (1mg/mL), the FluoroPOSS tended to migrate more towards the surface. Meanwhile, the surface roughness was also enhanced and thus the contact area will increase when the AFM slide across the surface, likely leading to the increase in friction coefficient at a high FluoroPOSS loading. Therefore, only a certain concentration of hydrophobic segment on the surface can enhance low friction.

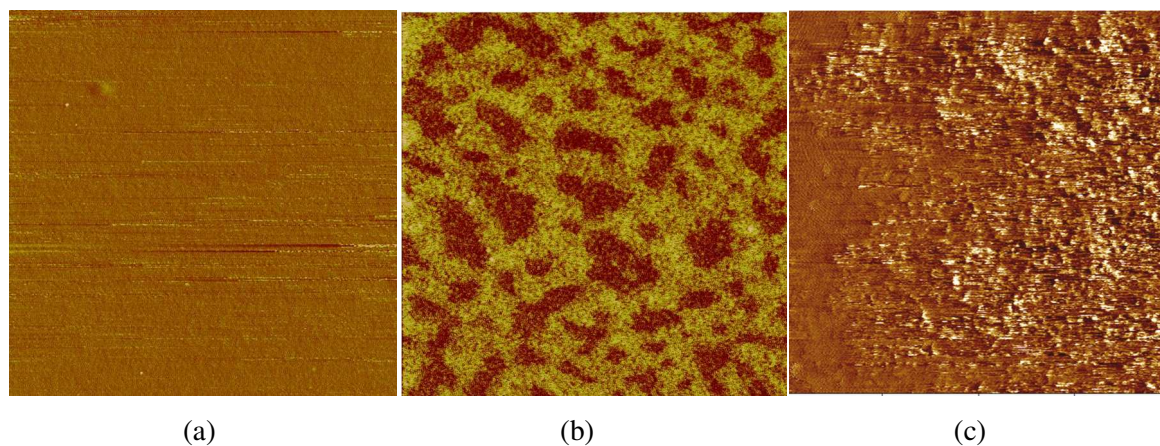


Figure 5. Typical phase images on different FluoroPOSS-PMMA blends. Scan size is $5 \times 5 \mu\text{m}$. The phase angle scale on the AFM images is 0° to 5° . The roughness for each film is given. (a) PMMA, $R_a = 0.56 \text{ nm}$ (b) **3a**: 0.3 mg/mL , $R_a = 1.02 \text{ nm}$ (c) **3a**: 1 mg/mL , $R_a = 2.24 \text{ nm}$ Scan size is $5 \times 5 \mu\text{m}$.

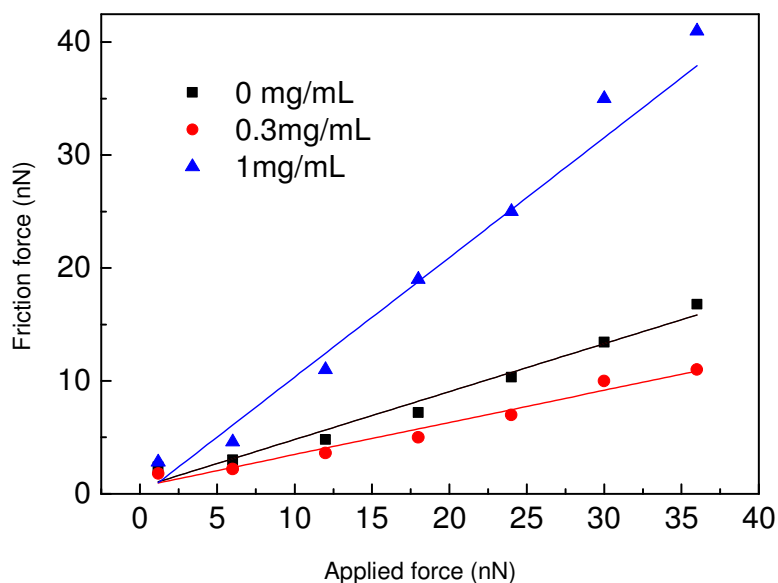


Figure 6.) Friction force vs. normal force for FluoroPOSS-PMMA blends.

Table 4. Summary on the friction coefficients of different FluoroPOSS/PMMA blends.

FluoroPOSS/PMMA solution	μ 0.0 mg/mL	μ 0.3 mg/mL	μ 1.0 mg/mL
3a /PMMA	0.425	0.409	1.265
3e /PMMA	0.425	0.375	1.458

Conclusion

In summary, we have synthesized five fluorinated POSS derivatives (**3a-3e**) by convenient hydrosilylation reaction. Compounds **3a**, **3d** and **3e** appear as fluidic oil at room temperature with melting point below $-80\text{ }^{\circ}\text{C}$. Compound **3e** has shown low evaporation loss with only 1.8% weight loss after heating at $218\text{ }^{\circ}\text{C}$ for 48 h. This is mainly ascribed to the much higher viscosity of **3e** compared with other FluoroPOSS samples. Integrating POSS core with fluorinated units not only considerably enhances the thermal stability of resulting fluorinated POSS derivatives, but also provide a type of unique POSS oils which is able to behave as effective lubricating materials. Furthermore, due to the relatively large size of the POSS core, the fluorine content in lubricant molecules will be considerably reduced without compromising their lubrication performance, offering the first category of fluorinated POSS oil. Blending of the fluorinated POSS samples with PMMA polymer has been conducted and it is found that incorporation of 5 wt.% of the FluoroPOSS sample into the PMMA matrix can enhance the hydrophobicity of the PMMA film with water contact angle increased from 68° for neat PMMA to more than 90° for FluoroPOSS/PMMA blend. AFM study is carried out to investigate the morphological changes after addition of FluoroPOSS. It is realized that addition of FluoroPOSS would increase the surface roughness of the PMMA film. The friction coefficient is slightly decreased after addition of small amount of FluoroPOSS (0.3 mg/mL) and increased after more FluoroPOSS is added (1 mg/mL). More effort in applying these FluoroPOSS oils as high performance lubricant under harsh conditions and as superhydrophobic coating materials is currently underway in our lab.

Acknowledgement

The authors would like to acknowledge the financial support from Science and Engineering Research Council (SERC), A*STAR (Grant No: 1324004089).

References

1. *Applications of polyhedral oligomeric silsesquioxanes, Advances in silicon science*, ed. Hartmann-Thompson C, Springer, 2011, vol. 3.
2. R. H. Baney, M. Itoh, A. Sakakibara and T. Suzuki, *Chem. Rev.*, 1995, **95**, 1409.

3. D. B. Cordes, P. D. Lickiss and F. Rataboul, *Chem. Rev.*, 2010, **110**, 2081.
4. R. M. Laine and M. F. Roll, *Macromolecules*, 2011, **44**, 1073.
5. R. M. Laine, *J. Mater. Chem.*, 2005, **15**, 3725.
6. K. L. Chan, P. Sonar and A. Sellinger, *J. Mater. Chem.*, 2009, **19**, 9103.
7. X. Wang, C. M. Cho, W. Y. Say, A. Y. X. Tan, C. He, H. S. O. Chan and J. Xu, *J. Mater. Chem.*, 2011, **21**, 5248.
8. R. Y. Kannan, H. J. Salacinski, P. E. Butler and A. M. Seifalian, *Acc. Chem. Res.*, 2005, **38**, 879.
9. J. Wu and P. T. Mather, *J. Macrom. Sci. Part C: Polym. Rev.*, 2009, **49**, 25.
10. K. Tanaka and Y. Chujo, *J. Mater. Chem.*, 2012, **22**, 1733.
11. R. W. J. M. Hanssen, R. A. van Santen and H. C. L. Abbenhuis, *Eur. J. Inorg. Chem.*, 2004, 675.
12. W. Zhang and A. H. E. Müller, *Prog. Polym. Sci.*, 2013, **38**, 1121.
13. (a) F. Wang, X. Lu and C. He, *J. Mater. Chem.*, 2011, **21**, 2775. (b) A. Pan, S. Yang, L. He and X. Zhao, *RSC Adv.*, 2014, **4**, 27857. (c) Y. -S. Lu and S. -W. Kuo, *RSC Adv.*, 2014, **4**, 34849.
14. *Hydrosilylation: a comprehensive review on recent advances. Advances in Silicon Science*, ed. B. Marciniec, Springer, 2009.
15. S. Ramirez and J. Mabry, in *Handbook of Fluoropolymer Science and Technology*, ed. D.W. Smith Jr., S. T. Iacono and S. S. Iyer, John Wiley & Sons, Inc., 2014.
16. S. S. Chhatre, J. O. Guardado, B. M. Moore, T. S. Haddad, J. M. Mabry, G. H. McKinley and R. E. Cohen, *ACS Appl. Mater. Interfaces*, 2010, **2**, 3544.
17. A. Tuteja, W. Choi, M. Ma, J. M. Mabry, S. A. Mazzella, G. C. Rutledge, G. H. McKinley, R. E. Cohen, *Science*, 2007, **318**, 1618.
18. A. Tuteja, W. Choi, J. M. Mabry, G. H. McKinley and R. E. Cohen, *Proc. Natl. Acad. Sci. U.S.A.*, 2008, **105**, 18200.
19. J. M. Mabry, A. Vij, S. T. Iacono, and B. D. Viers, *Angew. Chem. Int. Ed.*, 2008, **47**, 4137.
20. S. M. Ramirez, Y. J. Diaz, C. M. Sahagun, M. W. Duff, O. B. Lawal, S. T. Iacono and J. M. Mabry, *Polym. Chem.*, 2013, **4**, 2230.
21. W. Choi, A. Tuteja, S. Chhatre, J. M. Mabry, R. E. Cohen, G. H. McKinley, *Adv. Mater.*, 2009, **21**, 2190.

22. (a) J. Xu, X. Li, C. M. Cho, C. L. Toh, L. Shen, K. Y. Mya, X. Lu and C. He, *J. Mater. Chem.*, 2009, **19**, 4740. (b) B. Wang, Q. Lin, C. Shen, Y. Han, J. Tang and H. Chen, *RSC Adv.*, 2014, **4**, 52959. (c) L. Li, S. Feng and H. Liu, *RSC Adv.*, 2014, **4**, 39132. (d) H. Li, X. Zhao, G. Chu, S. Zhang and X. Yuan, *RSC Adv.*, 2014, Accepted Manuscript, DOI: 10.1039/C4RA07113A.
23. A. K. Kota, G. Kwon, W. Choi, J. M. Mabry and A. Tuteja, *Nat. Commun.*, 2012, **3**, 1025.
24. Non-symmetric, partially fluorinated lubricant additives, patent number: WO2000065002 A1.
25. (Fluorinated phenoxy)(3-perfluoroalkylphenoxy)-cyclic phosphazenes, patent number: US 5015405 A.
26. Phosphazene compound, lubricant and magnetic recording medium having such compound, method of preparation, and method of lubrication, patent number: WO2008008041 A1.
27. E. O. Dare, *Turk. J. Chem.*, 2006, **30**, 585.
28. X. Wang, J. M. Chin, C. He and J. Xu, *Sci. Adv. Mater.*, 2014, **6**, 1553.
29. S. Ebnesajjad, Chapter 4 in *Applied Plastics Engineering Handbook*, ed. M. Kutz, Elsevier Inc., 2011.
30. (a) C. Zhang and R.M. Laine, *J. Am. Chem. Soc.* 2000, **122**, 6979. U. (b) Dittmar, B. J. Hendan, U. Florke, H. C. Marsmann, *J. Organomet. Chem.* 1995, **489**, 185.
31. Y. C. Sheen, C. H. Lu, C. F. Huang, S. W. Kuo and F. C. Chang, *Polymer*, 2008, **49**, 4017.
32. K. W. Huang, L. W. Tsai and S. W. Kuo, *Polymer*, 2009, **50**, 4876.
33. Y. Ma, X. Cao, X. Feng, Y. Ma and H. Zou, *Polymer*, 2007, **48**, 7455.
34. P. J. Eaton, P. Graham, J. R. Smith, J. D. Smart, T. G. Nevell and J. Tsibouklis, *Langmuir*, 2000, **16**, 7887.
35. H. P. Mungse and O. P. Khatri, *J. Phys. Chem. C*, 2014, **118**, 14394.